Applied Catalysis B: Environmental 113–114 (2012) 281–289

Contents lists available at SciVerse ScienceDirect

Applied Catalysis B: Environmental

journal homepage: www.elsevier.com/locate/apcatb

Steam reforming of phenol–ethanol mixture over 5% Ni/Al_2O_3

Gabriella Garbarino[a], Vicente Sanchez Escribano[b], Elisabetta Finocchio[a], Guido Busca[a,*]

[a] Dipartimento di Ingegneria Chimica e di Processo, Università di Genova, P.le J.F. Kennedy 1, I-16129, Genova, Italy
[b] Dpto. de Química Inorgánica, Facultad de Ciencias Químicas, Universidad de Salamanca, Pl. de la Merced s/n, 37008 Salamanca, Spain

ARTICLE INFO

Article history:
Received 12 September 2011
Received in revised form
10 November 2011
Accepted 26 November 2011
Available online 6 December 2011

Keywords:
Biomass tar
Steam reforming
Nickel/alumina
Infrared spectroscopy
Phenol
Ethanol
Hydrogen

ABSTRACT

The steam reforming of 1:2 phenol–ethanol mixture (ca. 80 $g_{ph+eth}/N\,m^3$ in He) as a model of biomass gasification tar, has been investigated over Ni/Al_2O_3, $Ni/MgO-Al_2O_3$ and $Ni/ZnO-Al_2O_3$ catalysts. In this paper interest is focused over a 5% $Ni-Al_2O_3$ catalyst, that has been characterized in the unreduced and reduced states by IR of CO adsorbed at low temperature. The steam reforming reaction of ethanol and phenol has also been studied, separately, by IR spectroscopy. In spite of its low Ni content and the absence of alkali and alkali earth ions, this catalyst is actually active in the steam reforming of both ethanol and phenol. The reaction is, however, shifted to higher temperature than with catalysts containing higher Ni-loadings and also Mg and/or Zn ions. Ethanol steam reforming occurs at lower temperature than phenol steam reforming and does not seem to be much hindered by the presence of phenol. Phenol steam reforming in the presence of ethanol starts after, but is highly selective to CO_x and H_2. At low temperature, however, alkylation of phenol mainly occurs over the 5% $Ni-Al_2O_3$ catalyst to give mostly o-ethylphenol. Active ethoxide, acetate and phenate species are observed on the surface.

1. Introduction

Hydrogen is mostly produced today through steam reforming of hydrocarbons, usually natural gas [1,2], performed at 1000–1200 K. The industrial catalysts are based on Ni supported on an alumina-based carrier, usually stabilized by the presence of alkali and/or alkali earth cations.

The production of "biohydrogen", i.e. hydrogen arising from renewables, would result in the release of the energy production from fossil fuels and, simultaneously, in the reduction of greenhouse gases emissions. Several approaches can be applied to produce biohydrogen [3]. Among them, hydrogen and syngas may be produced by biomasses through a variety of pyrolysis and gasification processes [4]. Most of these processes are hampered by the coproduction of at least 10–50 $g/N\,m^3$ of tars, a mixture of heavy compounds that may result in fouling of heat exchangers and reactors. Studies report that phenol is the main component of tar after low temperature gasification [4,5]. Lighter organics are usually also present together with tars, that also act as primary source for larger molecules in biomass derived syngases. Ethanol is cited among such syngas impurities [6].

A steam reforming step is frequently considered to remove such noxious compounds. However, well established catalytic systems for biomass tar steam reforming is still lacking. Among active catalysts for this step [7], commercial methane steam reforming catalysts based on alkali-or alkali earth containing Ni/Al_2O_3 have been reported to be quite performant [8–10] and are commercially proposed by, e.g. Nextec [11] for this application. These catalysts are prone to deactivation by sulphur poisoning, coking and sintering [12], but can also be regenerated by steaming [13,14]. Noble metal catalysts, in particular Rh-based catalysts may be more active at low temperature and resistant to sulphur poisoning [15,16] but are obviously more expensive.

The steam reforming of phenol was recently investigated by Efstathiou and co-workers over natural materials [17], usually added in the gasification reactor to limit tar in the effluent, and over Rh based catalysts [18,19]. In our laboratories, a systematic investigation of tar steam reforming has been undertaken. To model tar feed we decided to mix phenol with ethanol. The addition of ethanol allows both to test a mixture of lighter and heavier compounds and to use a single tri-component liquid phase fed through a single HPLC pump into the reactor. The presence of ethanol in ethanol–phenol–water solutions allows to increase phenol-to-water mole ratio in a single liquid phase. A number of catalysts have been tested in our preliminary investigation. Here we will report results using 5% Ni/Al_2O_3 catalyst. The composition of this material, with such a low amount of nickel and the absence of alkali and alkali metals, is far from that of best catalysts. However, the use of

* Corresponding author. Tel.: +39 010 353 6024; fax: +39 010 353 6028.
E-mail address: Guido.Busca@unige.it (G. Busca).

0926-3373/$ – see front matter © 2011 Elsevier B.V. All rights reserved.
doi:10.1016/j.apcatb.2011.11.048

this catalyst allowed us to apply IR spectroscopy to study reactants adsorption, to investigate effect of loading and role of uncovered support surface, and to distinguish the effects of alkali and alkali earths on the reaction from those of the main catalysts components in the reaction.

2. Experimental

2.1. Catalyst preparation

5% Ni/Al_2O_3 catalyst (40 m^2/g) has been prepared by conventional wet impregnation of Siralox 1.5/40 support (alumina with 1.5% SiO_2 from Sasol) using Ni nitrate hexahydrate water solution. After impregnation, drying 363 K for 8 h and calcination at 973 K for 5 h have been performed. In the same way has been prepared, with the appropriate Ni amount a sample with 50% NiO (w/w), corresponding to 39% Ni (w/w) prepared with higher surface area alumina (170 m^2/g). The preparation of $Ni/MgO\text{-}Al_2O_3$ and $Ni/ZnO\text{-}Al_2O_3$ catalysts has been reported elsewhere [20].

2.2. Catalytic tests

The catalytic experiments were carried out in a fixed-bed tubular quartz flow reactor, operating isothermally, loaded with 44 mg of catalyst mixed with 440 mg of quartz particles (both of them 60–70 mesh sieved). The catalytic test were performed feeding 80 N ml/min containing 70% He (carrier gas), 27% water, 2% ethanol and 1% phenol mol/mol, corresponding to 84 g/N m^3 of ethanol + phenol, 42.9 g/N m^3 of phenol. The phenol–water–ethanol single phase liquid solution was pumped through a HPLC pump (Shimadzu Corp. LC-D10 AD) in an appropriate heating section at 673 K. After vaporization it is mixed to the carrier gas and fed to the reactor. The range of the temperatures of the reactor oven was varied from 773 K to 1073 K, and the results were reported in function of the measured temperature of the catalytic bed.

Products analysis was performed with a gas-chromatograph Agilent 4890 equipped with a Varian capillary column "Molsieve 5A/Porabond Q Tandem" and TCD and FID detectors in series. Between them a nickel catalyst tube was employed to reduce CO to CH_4. A six-port valve with a 0.5 cm^3 loop was used for the gas sampling of the outlet gases. The sampling of the outlet vapors was also made by injection, using a gas-tight with a nominal volume of 0.25 ml. A sampling injection point at the end of the vaporization zone allowed to analyse the reagents and to determine that the feed composition was not modified in the vaporization zone. Products analysis was also performed with a GC/MS (HP GCD plus), in order to have a precise identification of the compounds. Hydrogen was detected as a negative peak in the TCD detector signal of GC and also calculated on the basis of the C-product yields. The two measures were confirmed to be in reasonable agreement.

No catalyst pretreatments were performed. The results reported are based on reactant conversions, selectivity to carbon-containing products vs. temperature, as measured at each temperature when apparent steady state was reached, generally in 1 h. Reactant conversion is defined as follows:

$$X_{\text{react.}} = \frac{n_{\text{react.}}\text{in} - n_{\text{react.}}\text{out}}{n_{\text{react.}}\text{in}} \quad (1)$$

while selectivity to product i is defined as follows:

$$S_i = \frac{n_i}{\nu_i(n_{\text{react.}}\text{in} - n_{\text{react.}}\text{out})} \quad (2)$$

where n_i is the moles number of compound i, and ν_i is the ratio of stoichiometric reaction coefficients. When applied to the overall carbon feed, n_i is the carbon moles number of compound i, $n_{\text{react.}}$ is the carbon moles number of reactants mixture as a whole and $\nu_i = 1$.

2.3. IR studies

Pressed disks of the pure catalysts powders were activated "in situ" by using an infrared cell connected to a conventional gas manipulation/outgassing ramp. The catalyst disk was first submitted to a treatment in air for 30 min, followed by evacuation at 773 K before the adsorption experiments. In order to obtain the reduced catalyst, after the mentioned evacuation, it was put into contact with $H_2 \sim 400$ Torr at 773 K, for 30 min, and successively outgassed at the same temperature. CO adsorption was performed at 133 K by introducing a known dose of the gas (10 Torr) inside the low temperature infrared cell containing the previously activated wafers. IR spectra were collected using a Nicolet Nexus FT instrument, during evacuation upon warming at increasing temperatures between 133 K and 273 K.

Steam reforming studies have been performed in the IR cell by admitting controlled low pressures of the reactants at room temperature (ethanol 7 Torr + H_2O vapor 14 Torr for ethanol steam reforming, phenol 1 Torr + H_2O vapor 7 Torr for phenol steam reforming) then increasing temperature. Spectra of the gas and of the catalyst were recorded alternatively upon increasing temperature.

3. Results and discussion

3.1. Catalytic steam reforming of ethanol/phenol mixture

In Table 1 data on catalytic experiments are reported for the studied Ni-based catalysts. The data shown here refer to experiments done using the same conditions and the same furnace temperature, 873 K. The real measured bed temperature is also reported in the table.

The results show that the 5% Ni/Al_2O_3 catalyst is the least active, as expected indeed due to the lowest Ni content. With the other catalysts, more loaded with Ni, conversion at this furnace temperature approaches to unit value, with CO_2 and CO largely being the main C-containing products, together with hydrogen. Only a small amount of methane is also found with the higher Ni-loading samples. Only with the 5% Ni/Al_2O_3 catalyst several incomplete conversion products are found, such as ethylene, ethane,

Table 1
Carbon conversions and selectivities for steam reforming of ethanol–phenol mixture over different catalysts at T furnace = 873 K.

Catalyst	T furnace [K]	T bed [K]	C conversion	S_{CH_4}	S_{CO}	S_{CO_2}	$S_{CH_2CH_2}$	$S_{CH_3CH_3}$	S_{HCHO}	S_{CH_3CHO}	$S_{CH_3COCH_3}$	$S_{C_6H_6}$	$S_{(C_8+C_{10})}$
$Ni5\%/Al_2O_3$*	873	810	0.30	0.02	0.05	0.18	0.29	0.02	0.01	0.38	0.01	0.01	0.04
$Ni39\%/Al_2O_3$*	873	804	0.98	0.04	0.37	0.55	0.02	0.01	0.00	0.00	0.00	0.01	0.00
$Ni60\%\text{-}MgO\text{-}Al_2O_3$**	873	823	0.99	0.08	0.28	0.63	0.00	0.00	0.00	0.00	0.00	0.00	0.00
$Ni47\%\text{-}ZnO\text{-}Al_2O_3$**	873	824	0.99	0.08	0.24	0.68	0.00	0.00	0.00	0.00	0.00	0.00	0.00

* Ni% wt with respect to the support weight.
** Ni% wt with respect to the overall catalyst weight.

Table 2
Conversions and selectivities to C-containing products based on the single reactant for steam reforming of ethanol–phenol over Ni5%/Al_2O_3.

T bed [K]	Conversion and selectivities vs. ethanol										
	$X_{CH_3CH_2OH}$	S_{CH_4}	S_{CO}	S_{CO_2}	$S_{CH_2CH_2}$	$S_{CH_3CH_3}$	S_{HCHO}	S_{CH_3CHO}	$S_{CH_3COCH_3}$	S_{C_8}	$S_{C_{10}}$
721	0.86	0.00	0.00	0.04	0.20	0.00	0.00	0.22	0.03	0.43	0.07
810	0.64	0.02	0.06	0.18	0.30	0.03	0.01	0.40	0.01	0.01	0.00
901	0.64	0.15	0.07		0.40	0.01	0.00	0.37	0.00	0.00	0.00
951	0.96	0.03	0.97		0.00	0.00	0.00	0.00	0.00	0.00	0.00

T bed [K]	Conversion and selectivities vs. phenol						
	$X_{C_6H_5OH}$	S_{CH_4}	S_{CO}	S_{CO_2}	$S_{CH_6CH_6}$	S_{C_8}	$S_{C_{10}}$
721	0.90	0.00	0.00	0.00	0.00	0.82	0.18
810	0.03	0.00	0.00	0.00	0.16	0.84	0.00
901	0.53	0.00	0.95		0.05	0.00	0.00
951	0.99	0.00	1.00		0.00	0.00	0.00

formaldehyde, acetaldehyde, acetone and traces of benzene are observed, with also limited carbon conversion.

In Table 2 the effect of temperature on the reaction for the 5% Ni/Al_2O_3 catalyst are reported, where C-based conversion and selectivities are also calculated with respect to the single reactants, according to equations reported in Table 3. In fact, according to previous experience on ethanol steam reforming [20] and IR study of phenol conversion (see below), as well as in agreement with chemical considerations, methane, ethylene, ethane, formaldehyde, acetaldehyde and acetone are assumed to be products of ethanol conversion only (reactions (3)–(8) in Table 3). At the lowest temperatures, phenol conversion accounts for alkylation products only, by reaction with ethanol (reactions (12) and (13) in Table 3). Thus in these conditions also CO and CO_2 are assumed to be produced from ethanol only (reactions (1) and (2)). At higher temperatures the production of benzene is attributed to phenol hydrogenation (reaction (11)), while CO and CO_2 are the products of steam reforming of both reactants (reactions (1), (2), (9) and (10)). By difference, the CO + CO_2 sum can be attributed to the two reactants.

A very high conversion of both ethanol and phenol is found already at 721 K. However, as it can be seen in Table 2, phenol is actually fully converted into alkylate C8 and C10 compounds. Based on GC-MS the main alkylation product was found to be ortho-ethylphenol, with ethoxy-benzene, and 2,6-diethylphenol as minor products and also traces of para-ethylphenol. The relative amounts of these compounds are such that the yield to alkylates is 0.90 with respect to phenol, the yield to o-ethylphenol being 0.66, with 0.13 yield to 2,6-dialkylate, 0.09 yield to ethoxybenzene and 0.025 to the para isomer.

Alkylation of phenol by alcohols is an important reaction, even performed industrially, to produce alkylated phenols. This reaction is generally carried out over basic catalysts such as MgO and Fe–Mg oxides [21,22], but may also be catalyzed by solid acids such as alumina [23,24] and zeolites. On the other hand, according to Ballarini et al. [22] the reaction may be not simply catalyzed by acids and bases. Iron in fact has an important role in the alkylation of phenol by methanol over Fe–Mg oxides, where formaldehyde was found to act as an intermediate. Further investigations will be undertaken to go deeper on the possible role of nickel in our case.

This alkylation reaction actually tends to vanish at higher temperature and also with increasing Ni loading or, finally, by adding Mg or Zn to the catalyst formulation. In the context of tar abatement, it may be remarked that alkylation reaction can become relevant during non-steady-state conditions, such as during shut-down and start-up of the systems, producing heavier compounds instead of reducing them, from tar mixtures.

Additionally, ethanol is also converted into ethylene and acetaldehyde and, to a small extent, to CO and CO_2. By increasing temperature to 810 K the phenol alkylation reaction vanishes and conversion of phenol drops to near zero. Also ethanol conversion decreases, just because alkylation no more occurs, but still producing ethylene, acetaldehyde and carbon oxides. By further increasing reaction temperature, steam reforming of both ethanol and phenol occurs (Fig. 1). At 951 K both ethanol and phenol are almost totally steam reformed to give a mixture of CO and CO_2 together with hydrogen. The yield in hydrogen obtained at this temperature is very high, being really only limited by the incomplete conversion of CO in the water gas shift reaction. These data show that, in spite of its low Ni content and the absence of alkali and alkali earth ions, the catalyst is actually active in the steam reforming of both ethanol and phenol. The reaction is, however, shifted to higher temperature with respect to catalysts containing higher loadings of Ni and also Mg and/or Zn ions. The comparison with the results of ethanol steam reforming, i.e. performed in the absence of phenol, over the same catalysts [20], suggests that the presence of phenol actually does not inhibits significantly ethanol steam reforming, at least over high loading catalysts.

Table 3
Reactions used for mass balances.

$CH_3CH_2OH + H_2O \rightarrow 2CO + 4H_2$	(1)
$CH_3CH_2OH + 3H_2O \rightarrow 2CO_2 + 6H_2$	(2)
$CH_3CH_2OH \rightarrow C_2H_4 + H_2O$	(3)
$CH_3CH_2OH \rightarrow CH_3CHO + H_2$	(4)
$CH_3CH_2OH + 2H_2 \rightarrow 2CH_4 + H_2O$	(5)
$CH_3CH_2OH + H_2 \rightarrow C_2H_6 + H_2O$	(6)
$CH_3CH_2OH + H_2O \rightarrow 2HCHO + 3H_2$	(7)
$2CH_3CH_2OH \rightarrow CH_3COCH_3 + CO + 3H_2$	(8)
$C_6H_5OH + 5H_2O \rightarrow 6CO + 8H_2$	(9)
$C_6H_5OH + 11H_2O \rightarrow 6CO_2 + 14H_2$	(10)
$C_6H_5OH + H_2 \rightarrow C_6H_6 + H_2O$	(11)
$C_6H_5OH + CH_3CH_2OH \rightarrow CH_3CH_2{-}C_6H_4OH + H_2O$	(12)
$C_6H_5OH + 2CH_3CH_2OH \rightarrow (CH_3CH_2)_2{-}C_6H_3OH + 2H_2O$	(13)

3.2. Catalyst characterization by IR spectroscopy of low-temperature adsorption of CO

In Fig. 2 the spectrum of carbon monoxide adsorbed on the Siralox support is reported. In the left part of the figure the spectra are recorded after admission of CO into the cell at – 170 K and during outgassing upon warming. At the highest coverage the main maximum is at 2158 cm^{-1}. Looking at the OH stretching region (inset A) it is evident that this band is associated to the H-bonding of CO with surface hydroxy-groups. Upon this interaction, the band at 3740 cm^{-1} is involved partially, being shifted in part to near 3600 cm^{-1}. Thus the band at 2158 cm^{-1} is attributed to CO H-bonded on the terminal hydroxyl groups. In agreement with this

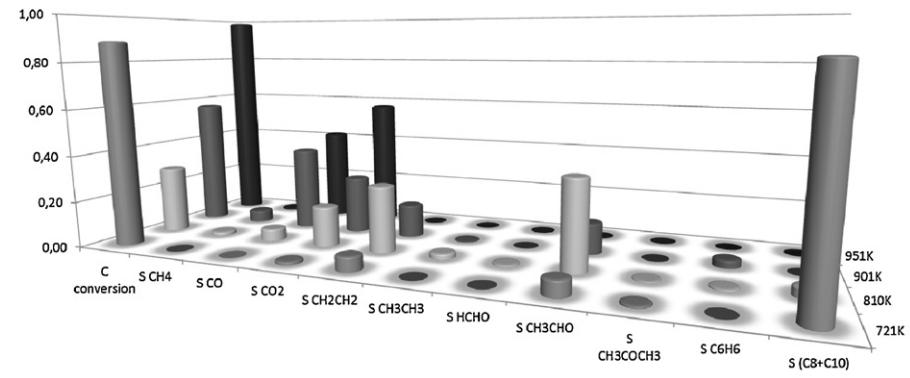

	C conversion	S CH4	S CO	S CO2	S CH2CH2	S CH3CH3	S HCHO	S CH3CHO	S CH3COCH3	S C6H6	S (C8+C10)
721K	0,89	0,00	0,00	0,01	0,06	0,00	0,00	0,07	0,01	0,00	0,84
810K	0,30	0,02	0,05	0,18	0,29	0,02	0,01	0,38	0,01	0,01	0,04
901K	0,57	0,05	0,37	0,26	0,15	0,00	0,00	0,13	0,00	0,03	0,00
951K	0,98	0,01	0,42	0,57	0,00	0,00	0,00	0,00	0,00	0,00	0,00

Fig. 1. Conversions (on C-basis) and selectivities (S) to C-containing products of ethanol/phenol mixture over 5% Ni-Siralox alumina catalyst as a function of reaction temperature.

assignment, this band disappears fast upon outgassing at low temperature.

A weaker feature, more resistant to outgassing, is observed at higher frequencies, with components near 2195 cm^{-1} and 2185 cm^{-1} the former more stable to outgassing (Fig. 2, inset B). They do not correspond to any perturbation of the νOH bands. They are assigned to CO species interacting with Lewis acidic Al^{3+} cations [25,26]. The shift with respect to νCO of gas or liquid CO is relatively weak, and this shows that after outgassing at 673 K only medium Lewis acidity ions are exposed, the strongest Lewis sites of alumina are still not produced, being the surface still in a highly hydroxylated state.

The spectra of surface species arising from CO adsorption over the unreduced 5% Ni/Al_2O_3 catalyst, at low temperature, are presented in Fig. 3. At the lowest temperature a main band is observed band at 2156 cm^{-1} assigned to CO adsorbed on the surface hydroxyl-groups. In fact, the analysis of the spectrum in the OH stretching region, reported in the inset in Fig. 3, shows a significant perturbation in particular of a component at 3730 cm^{-1}, which shifts down to 3600 cm^{-1}. The band at 2156 cm^{-1} and the perturbation of the OH stretching modes both disappear by outgassing upon warming, leaving a band at 2180 cm^{-1}, shifting during outgassing to above 2190 cm^{-1}, with a component just above 2200 cm^{-1}. Upon this experiment a band also grows at 2345 cm^{-1}, due to the asymmetric OCO stretching of molecularly adsorbed CO_2. This shows the oxidizing ability of the unreduced Ni/Al_2O_3, certainly due to Ni cations. This allows us to assign with confidence the band at 2180–2200 cm^{-1} to CO adsorbed on Al^{3+} ions [25,26], and on Ni^{2+} ions, like of NiO particles or $NiAl_2O_4$ [27,28] or dispersed Ni^{2+} oxide species [29,30].

The comparison of the spectra in the OH stretching region of the alumina support and the 5% Ni/Al_2O_3 catalyst (insets in Figs. 2 and 3) show that the impregnation process remarkably changes the spectrum with a broadening and perturbation of the bands of hydroxyl groups of alumina. This suggests that Ni species interact with surface OH's.

The spectra of surface species arising from CO adsorption over the reduced Ni/Al_2O_3 catalyst, at low temperature, are presented in Fig. 4. At the lowest temperature again the band of CO adsorbed on the surface hydroxyl-groups is observed band at 2156 cm^{-1}. By outgassing upon warming, a band at 2178–2190 cm^{-1} becomes more evident, shifting during outgassing to above 2190 cm^{-1}, with

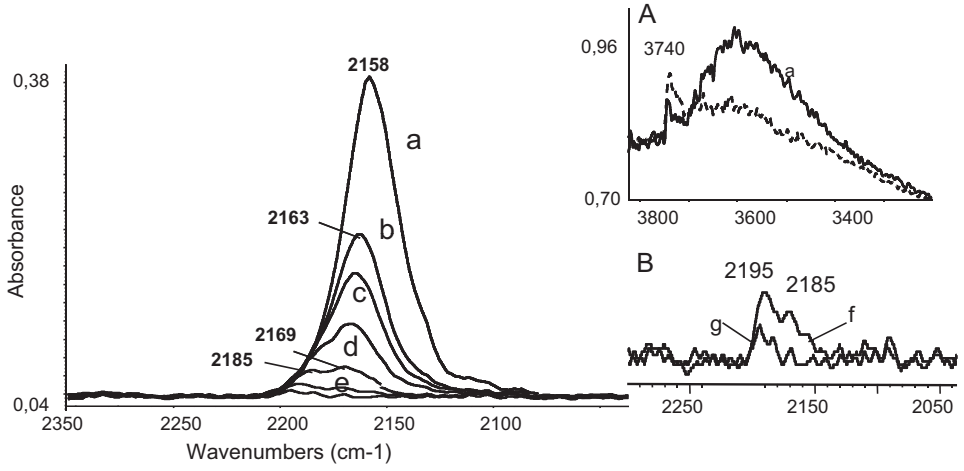

Fig. 2. FT-IR spectra of CO adsorbed over Siralox alumina activated by evacuation at 673 K, in the presence of CO (1 Torr) at 130 K and outgassing at increasing temperature (a: 130 K, b: 140 K, c: 150 K, d: 160 K, e: 170 K, f: 180 K, g: 190 K). Inset A: OH stretching region, activated sample (broken line), and after adsorption of CO at 130 K. Inset B: FT IR spectra recorded after CO adsorption and outgassing at 180 K and 190 K, expanded scale.

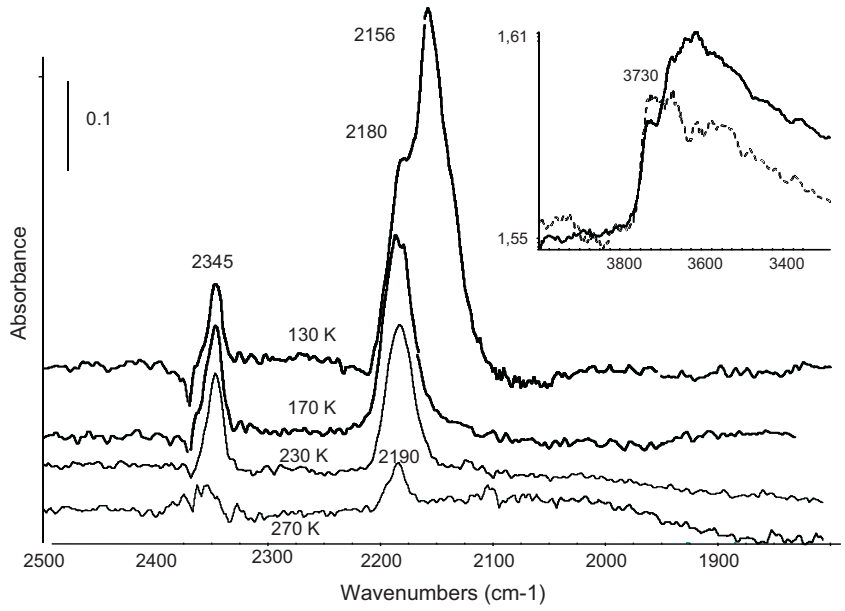

Fig. 3. FT-IR spectra of CO adsorbed over 5% Ni-Siralox alumina activated by evacuation at 673 K, in the presence of CO (1 Torr) at 130 K and after outgassing at increasing temperature from 130 to 273 K. Inset: OH stretching region of the activated sample (broken line) and after CO adsorption at 130 K.

a component just above 2200 cm^{-1}. This band is assigned again to CO adsorbed on Al^{3+} and Ni^{2+} ions, in agreement with the residual oxidizing ability of the reduced Ni/Al_2O_3, for which evidence is provided by the growth of the sharp band at 2345 cm^{-1}, due to adsorbed CO_2.

Additionally, a complex absorption is observed at lower frequencies, 2150–1900 cm^{-1}. Several quite sharp bands are observed in this region. They are superimposed to a broad absorption, more resistant to outgassing, centered at 2040 cm^{-1}, i.e. where CO stretchings of terminal carbonyls on metal particles typically occur.

The behaviour of the bands upon outgassing under warming suggests the existence of a doublet, at 2094 and 2132 cm^{-1}, associated to a slightly more labile species, and a triplet at 2010, 2040 and 2060 cm^{-1}, assigned to a slightly more resistant species. The doublet at 2094 and 2132 cm^{-1} could be associated with the formation of $Ni^{+}(CO)_2$ complexes, which are typically characterized by adsorption bands at 2100–2081 cm^{-1} and 2145–2130 cm^{-1} [25,31]. In the region 2000–2100 cm^{-1} the three weak bands at 2010, 2040 and 2060 cm^{-1}, with similar relative intensities, could be due to Ni^0 polycarbonyls, like $Ni(CO)_3$, likely frozen precursors of the formation of $Ni(CO)_4$.

As said, the most stable species is characterized by a broad band at 2040 cm^{-1} typical of terminal carbonyls on reduced metal centers. No evidence is found for bridging species. This suggests that atomically dispersed Ni atoms or very small clusters are formed. In fact CO adsorption on extended Ni metal particles usually gives rise to low-frequency CO stretching bands in the region of bridging and triply bridging CO together with and more intense than those due to terminal ones [32]. On Ni{1 1 1} at low coverage a predominant band is observed shifting from 1830 and 1900 cm^{-1} depending on the coverage, assigned to bridging CO, and a weaker one at 1796–1825 cm^{-1} attributed to hollow adsorbed molecules (triply

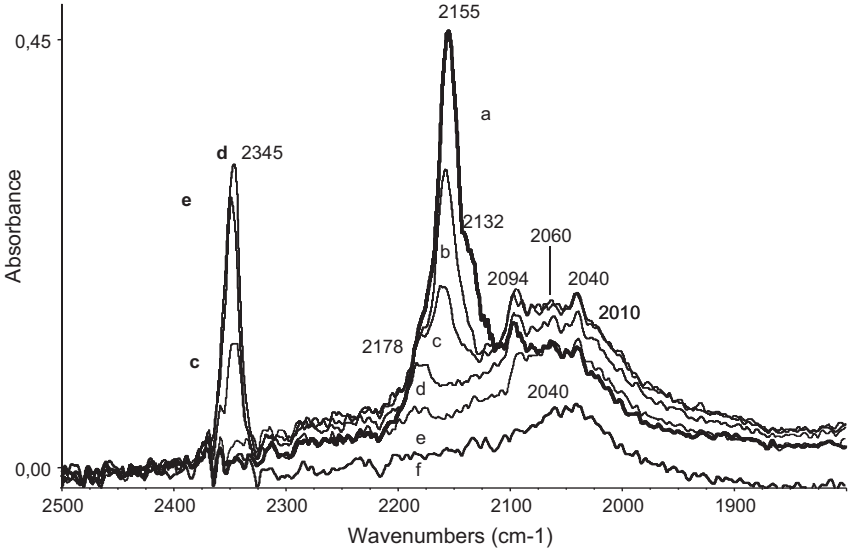

Fig. 4. FT-IR spectra of CO adsorbed over 5% Ni-Siralox alumina after reduction in hydrogen and evacuation at 673 K, in the presence of CO (1 Torr) at 130 K and after outgassing at increasing temperature (a: 130 K, b: 140 K, c: 150 K, d: 160 K, e: 210 K, f: 250 K).

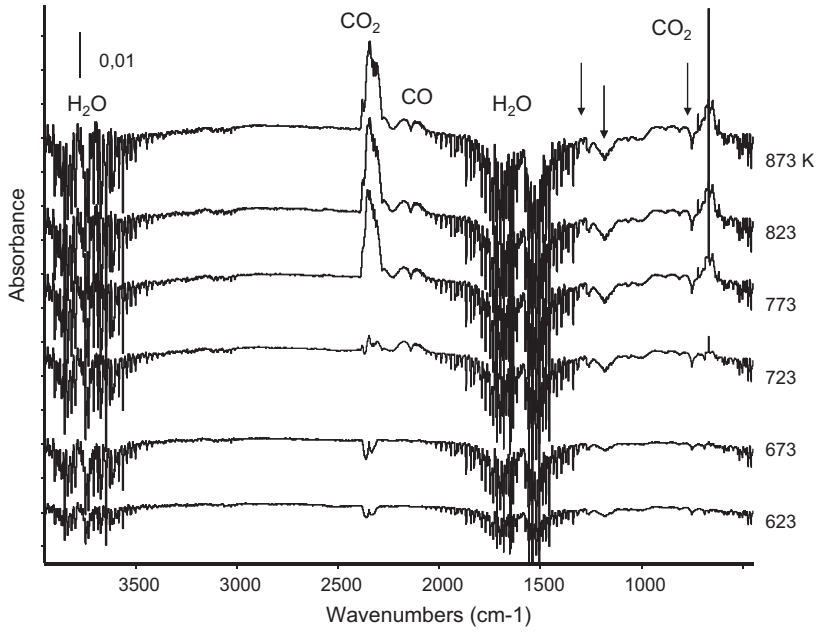

Fig. 5. FT-IR subtraction spectra of gas phase species arising from phenol and water co-adsorption and thermal evolution over hydrogen-reduced 5% Ni-Siralox alumina. Arrows: negative bands due to phenol consumption. The spectrum of phenol/water vapor mixture at room temperature has been subtracted.

bridging) together with weak bands due to terminal carbonyls (2030–2060 cm^{-1} depending on the coverage [32]). In fact more recent structural studies [33,34] show that at increasing coverage a sequence of different ordered structures, namely $p(2 \times 2)$-(CO), $\sqrt{3} \times \sqrt{3}$-$R30°$-(CO) and $c(2 \times 4)$-(2CO), all implying only triply bridging species (hcp and fcc positions) occurs. A recent DFT study [35] suggested that at half coverage the two low frequency bands can be due to in-phase and out-of-phase modes of these structures. Only at higher coverage ($\theta > 0.50$) a structure with one on top and three bridging species form. Similarly, also on Ni{1 0 0} [36,37] and on Ni{3 1 1} [38] the bands of terminal and bridging CO are observed together. Also in the case of reduced supported Ni catalysts the band of bridging CO is usually prominent [29,30,39]. The full absence of bands in the region below 2000 cm^{-1} here may be indication of the existence of atomically dispersed zerovalent nickel, together with unreduced cations, in our mildly reduced and low-loading Ni/Al_2O_3 sample. In fact, in agreement with the high support surface area and the low Ni loading dispersion of Ni on this catalyst is very high. Highly dispersed Ni ions are also quite refractory to reduction.

The IR spectra also show that surface hydroxyl groups are present on both reduced and unreduced surface not only up to 673 K (see inserts in Figs. 2 and 3) but also at least up to 973 K, at least. Appropriate experiments have shown that the treatment with water at high temperature does not modify significantly the spectrum in the OH stretching region.

3.3. IR study of phenol steam reforming

Steam reforming of phenol has been performed in the IR cell. The catalyst, previously mildly reduced as above, has been put into contact with phenol and water vapors at r.t. Then the temperature has been progressively increased up to 873 K. Both the spectra of the gas and of the catalyst have been recorded during heating in phenol and water vapors. The difference spectra of the gas phase recorded during this experiment are reported in Fig. 5. The gas-phase spectrum at room temperature has been subtracted from the spectrum recorded at increasing temperature. Up to 673 K only gas-phase phenol (see the bands at 1270, 1184, 751 cm^{-1}) and water have been detected. At 723 K, gas phase CO was found while the bands of both phenol and water definitely decreased in intensity, being well evident as negative bands in the subtraction spectra. Starting from 773 K only CO and CO_2 were detected in the gas phase together with water vapor. The spectrum of phenol was fully disappeared (arrows in Fig. 5 evidencing negative phenol bands). No bands of C-containing species except phenol, CO and CO_2 were found in the gas phase.

The surface species detected over the catalyst during the experiment are shown in Fig. 6. The spectra are interpreted in agreement with previous studies of IR spectra of phenol [40]

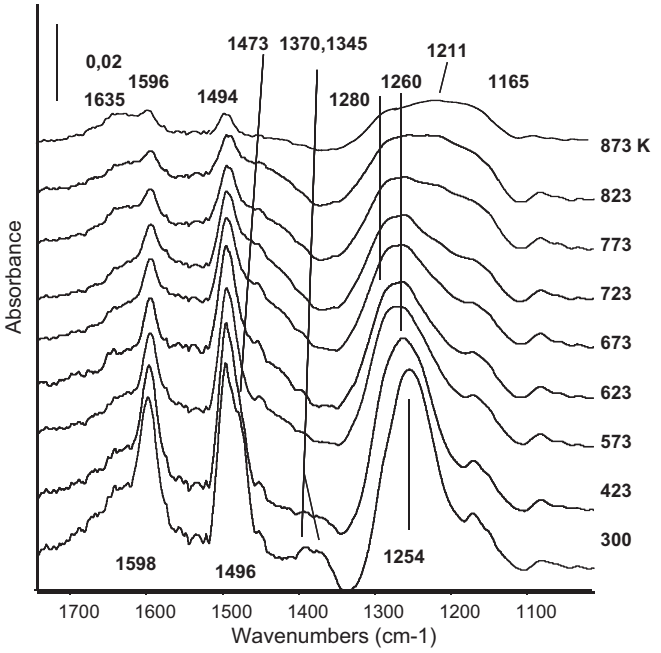

Fig. 6. FT-IR subtraction spectra of surface species arising from phenol and water co-adsorption and thermal evolution over hydrogen-reduced 5% Ni-Siralox alumina. The activated surface spectrum has been subtracted.

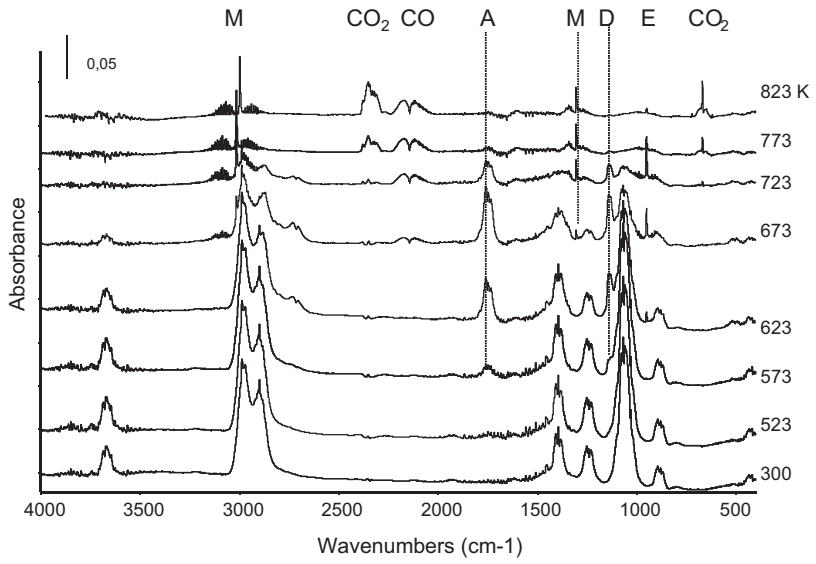

Fig. 7. FT-IR spectra of gas phase species arising from ethanol and water co-adsorption and thermal evolution over hydrogen-reduced 5% Ni-Siralox alumina. M = methane, D = diethyl ether, E = ethane, A = acetaldehyde.

and of phenol adsorbed on oxide catalysts [41] including alumina [42]. After contact at r.t. the spectrum seems to be dominated by the features of phenate species (1598 cm^{-1}, 8a ring vibration, 1496 cm^{-1}, 19a ring vibration, 1254 cm^{-1} C—O stretching), but with copresence of un-dissociated phenol (1473 cm^{-1}, 19a ring vibration, 1370, 1345 cm^{-1}, split in-plane OH deformation). At higher temperature, un-dissociated phenol disappears, while CO stretching of phenate species shifts to 1260 cm^{-1}. These band decrease in intensity, likely due to phenol desorption. The spectrum changes above 723 K, where it becomes more similar to that reported for phenol adsorption on alumina [42] where two types of phenate species where found, terminal, and bridging. The main band at 1280 cm^{-1} is assigned to CO stretching of terminal phenates on alumina, while the broader component at lower frequency (1250–1165 cm^{-1}) should contain the CO stretching of bridging phenates. The very broad absorption that is observed even at 873 K in the range 1300–1150 cm^{-1} and the persistence of the two bands near 1596 and 1494 cm^{-1}, together with the formation of a band at 1635 cm^{-1} (possibly due to COO stretching of carboxylate species) suggest that very stable aromatic oxygenated species form, likely over the alumina surface, which are refractory to steam reforming. On the contrary, the active adsorbed species for steam reforming are likely phenate species interacting with Ni species, supposed to be responsible for CO stretching at 1260 cm^{-1}, i.e. the most evident species until 723 K.

Summarizing, the IR study of phenol steam reforming suggests that the reaction occurs at the expense of surface phenate species adsorbed on Ni centers. These species start to be reactive above

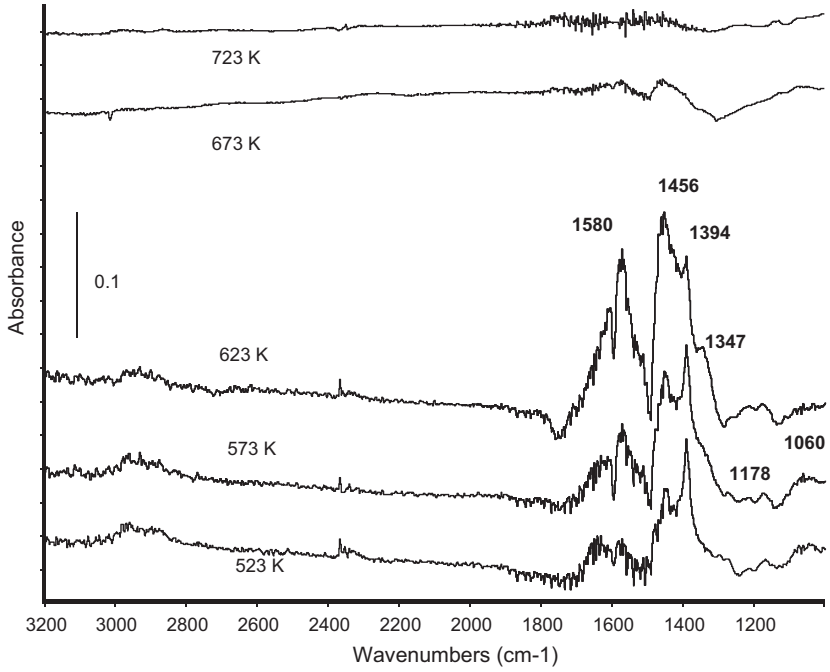

Fig. 8. FT-IR subtraction spectra of surface species arising from ethanol and water co-adsorption and thermal evolution over hydrogen-reduced 5% Ni-Siralox alumina. The activated surface spectrum has been subtracted.

673 K in the presence of water giving rise to CO and hydrogen. No evidence is found for intermediates or by-products from this reaction. Phenate species on alumina appear to be inactive spectators, while traces of carboxylate species are only found the very high temperature, possibly being also located on alumina and inactive in the reaction.

As remarked above, IR spectra also show that in conditions where reaction occurs, surface hydroxyl groups are present on the surface while molecular water is not observed. It seems likely that these species are active in the steam reforming reaction, as previously proposed for the reaction occurring on rhodium catalysts [43].

3.4. IR study of ethanol steam reforming

Steam reforming of ethanol has been performed in the IR cell. The catalyst, previously mildly reduced as above, has been put into contact with ethanol and water vapors at r.t. Then the temperature has been progressively increased up to 823 K.

The spectra of the gas phase recorded during this experiment are reported in Fig. 7. Up to 523 K only the spectrum of ethanol and water vapors were found. At 573 K small amounts of acetaldehyde (C═O stretching at 1746 cm^{-1}, PQR shape, CH stretching at 2715 cm^{-1}, PR shape) and diethylether (C—O—C stretching at 1137 cm^{-1}, PR shape) and traces of ethylene (CH_2 wagging at 950 cm^{-1}) are also evident. Ethylene band rises its maximum intensity at 723 K, then decreases without disappearing. Diethylether bands have their maximum intensities at 673–723 K and are still present in traces at 823 K. Acetaldehyde bands reach their maximum intensity at 673 K, decrease in intensity at 723 K and are disappeared at 773 K. Both CO (2142 cm^{-1}, PR shape) and methane (3016 and 1305 cm^{-1}) start to grow at 673 K, while CO_2 (2349 cm^{-1}, PR shape) starts to grow at 773 K.

The spectra of the corresponding surface species are reported in Fig. 8. Adsorption of ethanol at room temperature gives rise to the formation of a multiple absorption with maxima at 1394 (δ_{sym} CH_3) and at 1449 cm^{-1} (δ_{as} CH_3), due to the deformation modes of the CH bonds, and bands at 1178 and 1060 cm^{-1} which can be attributed to the asymmetric stretching modes of the C—C—O system of ethoxide groups [44]. Starting from 573 K a couple of new well evident bands appears at 1580 and 1456 cm^{-1}, with an additional weak and sharp component at 1347 cm^{-1}. These bands can be assigned confidently to acetate species (asymmetric and symmetric COO stretching, and CH_3 deformation), and grow at the expense of the bands of ethoxy groups. Under heating above 623 K the bands of acetate species start to apparently decrease in intensity while the sample absorbs more and more. This may either be due to a more complete reduction and syntering of the Ni particles or to some coking.

The results reported here confirm previous studies of ethanol steam reforming [20,45–47], showing that the evolution of surface ethoxy groups produced by dissociative adsorption of ethanol results essentially in the formation of ethylene, diethylether and acetaldehyde, occurring mostly in a lower temperature range, 573–623 K in the IR experiment. Surface acetate species also develop at the expense of surface ethoxides and their evolution appears to be associated to the formation of methane and CO mostly occurring at 673 K and above.

4. Conclusions

IR spectra of carbon monoxide adsorbed on our 5% Ni/Al_2O_3 catalyst show that, according to the low metal loading, our catalyst in the oxidized state is essentially constituted by highly dispersed Ni^{2+} ions on the alumina surface. Nickel, whose loading is over this catalyst comparable to that of a theoretical monolayer, seems to interact in particularly with surface hydroxyl groups whose IR spectrum is significantly perturbed.

Treatment in hydrogen in the IR cell actually only partially reduces Ni to metal, producing also partially reduced centers, possibly Ni^+, available to produce polycarbonyls with CO. Zerovalent Ni centers only adsorb CO producing terminal species, characterized by CO at 2040 cm^{-1}. No bridging species are observed. This suggests that extended metal particles (where adsorption of CO usually produces also bridging species) are not formed, only atomically dispersed Ni or very small clusters being detected.

In spite of the low Ni loading, the catalyst is active in the steam reforming of ethanol and phenol, converting almost completely phenol and ethanol into CO, CO_2 and hydrogen and small amounts of methane at 951 K. This temperature is of interest for biomass tar abatement, taking also into account the likely deactivation by sulphur of Ni-catalysts in practical commercial conditions. However, highly loaded Ni/Al_2O_3 catalysts are active at definitely lower temperatures, allowing almost total conversion of both ethanol and phenol already near 800 K.

Interestingly, our 5% Ni/Al_2O_3 catalyst shows at low temperature phenol alkylation activity. This reaction actually tends to vanish at higher temperature and also with increasing Ni loading or, finally, by adding Mg or Zn to the catalyst formulation. However, it may be remarked that this reaction can become relevant during non-steady-state conditions, such as during shut-down and start-up of the systems, producing heavier compounds instead of reducing them, from tar mixtures.

The catalytic results show that ethanol steam reforming occurs before phenol steam reforming and does not seem to be much hindered by the presence of phenol. Phenol steam reforming in the presence of ethanol starts after, but is highly selective to CO_x and H_2, without the evident formation of by-products. In particular, this is true when high Ni-loading catalysts are used. Surface ethoxide and phenate species seem to be involved in the reactions, possibly with surfaces hydroxyl-groups, while a significant role of surface acetate species in ethanol steam reforming is confirmed by IR experiments.

Acknowledgment

EF acknowledges the University of Genova, Italy “Progetto di Ricerca di Ateneo 2010 Ricercatori Universitari” for partially funding this research.

References

[1] J.R. Røstrup-Nielsen, J. Sehested, J.K. Norskov, Adv. Catal. 47 (2002) 66–139.
[2] R.M. Navarro, M.A. Peña, J.L.G. Fierro, Chem. Rev. 107 (2007) 3952–3992.
[3] E. Kırtay, Energy Conv. Manag. 52 (2011) 1778–1789.
[4] G.W. Huber, S. Iborra, A. Corma, Chem. Rev. 106 (2006) 4044–4098.
[5] J. Han, H. Kim, Renew. Sust. Energy Rev. 12 (2008) 397–416.
[6] T.A. Milne, R.J. Evans, N. Abatzoglou, Biomass gasifier “tars”: their nature, formation, and conversion, November 1998, NREL/TP-570-25357, available on internet.
[7] M.M. Yung, W.S. Jablonski, K.A. Magrini-Bair, Energy Fuels 23 (2009) 1874–1887.
[8] J. Corella, J.M. Toledo, R. Padilla, Ind. Eng. Chem. Res. 43 (2004) 2443–2445.
[9] J. Corella, A. Orıo, J.-M. Toledo, Energy Fuels 13 (1999) 702–709.
[10] C. Pfeifer, H. Hofbauer, Powder Technol. 180 (2008) 9–16.
[11] http://www.nextechmaterials.com.
[12] J. Sehested, Catal. Today 111 (2006) 103–110.
[13] L. Li, C.J. Howard, D.L. King, M.A. Gerber, R.A. Dagle, B.J. Stevens, US Patent Application 20110039686 (2011) to Battelle Mem. Inst.
[14] S.M. Hashemnejad, M. Parvari, Chin. J. Catal. 32 (2011) 273–279.
[15] M. Asadullah, T. Miyazawa, S. Ito, K. Kunimori, K. Tomishige, Green Chem. 5 (2003) 399–403.
[16] H. Rönkkönen, P. Simell, M. Reininkainen, M. Niemelä, O. Krause, Fuel Proc. Technol. 92 (2011) 1457–1465.
[17] D.A. Constantinou, J.L.G. Fierro, A.M. Efstathiou, Appl. Catal. B: Environ. 95 (2010) 255–269.
[18] D.A. Constantinou, A.M. Efstathiou, Appl. Catal. B: Environ. 96 (2010) 276–289.
[19] K. Polychronopoulou, K. Giannakopoulos, A.M. Efstathiou, Appl. Catal. B: Environ., (2011) doi:10.1016/j.apcatb.2011.10.019, in press.

[20] C. Resini, T. Montanari, L. Barattini, G. Ramis, G. Busca, S. Presto, P. Riani, R. Marazza, M. Sisani, F. Marmottini, U. Costantino, Appl. Catal. A: Gen. 355 (2009) 83–93.
[21] H.-G. Franck, J.W. Stadelhofer, Industrial Aromatic Chemistry, Springer Verlag, Berlin, 1988.
[22] N. Ballarini, F. Cavani, L. Maselli, A. Montaletti, S. Passeri, D. Scagliarini, C. Flego, C. Perego, J. Catal. 251 (2007) 423–436.
[23] J. Spivey, Catalysis, Specialist Periodical Report, RSC, 23 (2011), 10–11.
[24] D.L.E. Winkler, R.H. Mortimer, Alkylation of phenolic compounds – United State Patent No. 2448942 (1948).
[25] K. Hadjiivanov, G.N. Vayssilov, Adv. Catal. 47 (2002) 307–511.
[26] T. Montanari, L. Castoldi, L. Lietti, G. Busca, Appl. Catal. A: Gen. 400 (2011) 61–69.
[27] G. Busca, V. Lorenzelli, V. Sanchez Escribano, R. Guidetti, J. Catal. 131 (1991) 167–177.
[28] G. Busca, V. Lorenzelli, V. Sanchez Escribano, Chem. Mater. 4 (1992) 595–605.
[29] C. Resini, T. Venkov, K. Hadjiivanov, S. Presto, P. Riani, R. Marazza, G. Ramis, G. Busca, Appl. Catal. A: Gen. 353 (2009) 137–143.
[30] M. Garcia-Diéguez, E. Finocchio, M.A. Larrubia, L.J. Alemany, G. Busca, J. Catal. 274 (2010) 11–20.
[31] K. Hadjiivanov, H. Knözinger, M. Mihaylov, J. Phys. Chem. B 106 (2002) 2618–2624.
[32] M.A. Vannice, in: J.R. Anderson, M. Boudart (Eds.), Catalysis, Science and Technology, vol. 3, Springer Verlag, 1982, pp. 139–198.
[33] G. Held, J. Schuler, W. Sklarek, H.-P. Steinrück, Surf. Sci. 398 (1998) 154–171.
[34] W. Braun, H.-P. Steinrück, G. Held, Surf. Sci. 575 (2005) 343–357.
[35] A. Eichler, Surf. Sci. 526 (2003) 332–340.
[36] J. Yoshinobu, M. Kawai, Surf. Sci. 363 (1996) 105–111.
[37] V. Formoso, A. Marino, G. Chiarello, R.G. Agostino, T. Caruso, E. Colavita, Surf. Sci. 600 (2006) 1456–1461.
[38] P. Schilbe, S. Siebentritt, K.-H. Rieder, Chem. Phys. Lett. 233 (1995) 569–574.
[39] A. Infantes-Molina, J. Mérida-Robles, P. Braos-García, E. Rodríguez-Castellón, E. Finocchio, G. Busca, P. Maireles-Torres, A. Jiménez-López, J. Catal. 225 (2004) 479–488.
[40] J.C. Evans, Spectrochim. Acta 16 (1960) 1382–1392.
[41] G. Busca, G. Ramis, V. Lorenzelli, Stud. Surf. Sci. Catal. 55 (1990) 825–832.
[42] A. Popov, E. Kondratieva, J.P. Gilson, L. Mariey, A. Travert, F. Maugé, Catal. Today 172 (2011) 132–235.
[43] K. Polychronopoulou, A.M. Efstathiou, Catal. Today 116 (2006) 341–347.
[44] S.C. Street, A.J. Gellmann, Colloids Surf. A: Physicochem. Eng. Aspects 105 (1995) 27.
[45] C. Resini, M.C. Herrera Delgado, S. Presto, L.J. Alemany, P. Riani, R. Marazza, G. Ramis, G. Busca, Int. J. Hydrogen Energy 33 (2008) 3728–3735.
[46] L. Barattini, G. Ramis, C. Resini, G. Busca, M. Sisani, U. Costantino, Chem. Eng. J. 153 (2009) 43–49.
[47] G. Busca, U. Costantino, T. Montanari, G. Ramis, C. Resini, M. Sisani, Int. J. Hydrogen Energy 35 (2010) 5356–5366.